

Exclusive Decays of $B \rightarrow K^{(*)}l^+l^-$ in the PQCD

Chuan-Hung Chen^a and C. Q. Geng^b

^a*Department of Physics, National Cheng Kung University
Tainan, Taiwan, Republic of China*

^b*Department of Physics, National Tsing Hua University
Hsinchu, Taiwan, Republic of China*

Abstract

We study the exclusive decays of $B \rightarrow K^{(*)}l^+l^-$ within the framework of the PQCD. We obtain the form factors for the $B \rightarrow K^{(*)}$ transitions in all allowed values of q^2 , which agree with the lattice results. We find that our distributions of the decay rates and leptonic asymmetries are consistent with that given in the other QCD models in the literature.

1 Introduction

The recent CLEO measurement of the radiative $b \rightarrow s\gamma$ decay [1] has motivated theorists to study exclusive rare B meson decays such as $B \rightarrow K^{(*)}l^+l^-$ [2]. In the standard model, these rare decays occur at loop level and provide us with information on the parameters of the Cabibbo-Kobayashi-Maskawa (CKM) matrix elements [3] as well as various hadronic form factors. In this paper, we examine the decays of $B \rightarrow (K, K^*)l^+l^-$ within the framework of the perturbative QCD (PQCD).

The calculations of matrix elements for exclusive hadron decays can be performed in the PQCD approach developed by Brodsky-Lepage (BL) [4]. The application to B meson decays was first carried out in Refs. [5] and [6]. In the BL formalism, the nonperturbative part is expressed as the hadron wave functions which could be determined via various QCD models such as the QCD sum rule method or lattice gauge theory and the transition amplitude is factorized into the convolution of hadron wave functions and the hard amplitude of the constituent quarks. However, with the BL approach, the nonperturbative effects appear [7, 8] if one of the constituent quarks carries nearly all the momentum of hadron. To solve the problem, Li and Stermann [9] proposed by including the transverse momentum of constituent quark, k_T , and the Sudakov form factor to the wave functions to suppress the soft contributions from higher order corrections. In terms of the parameter b with b being the conjugate variable of k_T , they also showed that the effects can be also expressed as that in the BL factorization formalism.

The modified PQCD factorization theorem for exclusive heavy meson decays has been developed some time ago [10, 11, 12] and applied to nonleptonic $B \rightarrow D^{(*)}\pi(\rho)$ [10], penguin induced radiation $B \rightarrow K^*\gamma$ [13], and $B \rightarrow KK$ [14] decays. These decays involve three scales: the M_W scale as the initial condition of renormalization-group (RG) equation, the typical scale t which reflects the specific dynamics of the heavy meson decays, and the factorization scale $1/b$. Above the factorization scale, there are two large logarithms $\ln(M_W/t)$ and $\ln(tb)$, generated from radiative corrections. The former gives the evolution from M_W down to t described by the Wilson coefficient (WC), while the latter from t to $1/b$. There also exist double logarithms $\ln^2(Pb)$ arising from the radiative correction to the meson wave function, where P is the dominant light-cone component of a meson momentum. Resuming these double logarithms leads to a Sudakov form factor of $\exp(-s(P, b))$ which suppresses the long-distance contributions in the large b region such that the applicability of the PQCD around the energy scale of the bottom quark mass could be guaranteed.

The typical three-scale factorization formula is generally written as the following convolution product

$$C(t) \otimes H(t) \otimes \phi(x, b) \otimes \exp\left(-s(P, b) - 2 \int_{1/b}^t \frac{d\bar{\mu}}{\bar{\mu}} \gamma(\alpha_s(\bar{\mu}))\right) \quad (1)$$

where $C(t)$, $H(t)$ and $\phi(x, b)$ denote the WC, hard decay amplitude and non-perturbative wave function, respectively, and the quark anomalous dimension $\gamma = -\alpha_s/\pi$ is evaluated from t to $1/b$. Except $\phi(x, b)$ dictated by non-perturbative dynamics, all the convolution factors in Eq. (1) are calculable. Note that differing from the conventional factorization assumption (FA), the WC is also one of the convolution parts in Eq. (1). Thus, the μ dependent problem occurring in the FA could be solved naturally in the three-scale factorization formula.

The paper is organized as follows. In Sec. 2, we study the form factors in the framework of the PQCD for the decays of $B \rightarrow K^{(*)}$ transitions. In Sec. 3, we derive the forms of

the differential decay rates and lepton asymmetries for $B \rightarrow K^{(*)}l^+l^-$ based on the PQCD. In Sec. 4, we give the numerical analysis. We will also compare our results in the PQCD approach with that in the other QCD models. In Sec. 5, we present our conclusions.

2 Form factors in the framework of the PQCD

In the decay of $B \rightarrow Hl^+l^-$, the momentum of B (H) in the light-cone coordinate is chosen as $P_1 = (P_{1(2)}^+, P_{1(2)}^-, \mathbf{0}_T)$, where $P_1^\pm = M_B/\sqrt{2}$ and $P_2^\pm = (E_H \pm P_H)/\sqrt{2}$ with $E_H = (M_B^2 + M_H^2 - q^2)/2M_B$, $P_H = \sqrt{E_H^2 - P_H^2}$, and q^2 is the squared momentum transfer. We define the momentum of the light valence quark in the B meson as k_1 and use $x_1 = k_1^+/P_1^+$ with k_1^+ and k_{1T} being the plus and transverse components of k_1 , respectively. The two light valence quarks in the H meson carry the longitudinal momenta x_2P_2 and $(1-x_2)P_2$, and transverse momenta \mathbf{k}_{2T} and $-\mathbf{k}_{2T}$, respectively.

The Sudakov resummations of large logarithmic corrections lead to the exponential forms of $\exp(-S_B)$ and $\exp(-S_H)$ for B and H wave functions, respectively, where

$$\begin{aligned} S_B(t) &= s(x_1P_1^+, b_1) + 2 \int_{1/b_1}^t \frac{d\bar{\mu}}{\bar{\mu}} \gamma(\alpha_s(\bar{\mu})) , \\ S_H(t) &= s(x_2P_2^+, b_2) + s((1-x_2)P_2^+, b_2) + 2 \int_{1/b_2}^t \frac{d\bar{\mu}}{\bar{\mu}} \gamma(\alpha_s(\bar{\mu})) . \end{aligned} \quad (2)$$

In Eq. (2), b_1 and b_2 represent the transverse momentum extents of B and H and are conjugate to the parton transverse momenta k_{1T} and k_{2T} , respectively. The form for s is written as [15, 16, 9]

$$s(Q, b) = \int_{1/b}^Q \frac{d\mu}{\mu} \left[\ln \left(\frac{Q}{\mu} \right) A(\alpha_s(\mu)) + D(\alpha_s(\mu)) \right] , \quad (3)$$

where the anomalous dimensions A and D calculated to the two and one-loop levels, respectively, are given by

$$\begin{aligned} A &= C_F \frac{\alpha_s}{\pi} + \left[\frac{67}{9} - \frac{\pi^2}{3} - \frac{10}{27}f + \frac{2}{3}\beta_0 \ln \left(\frac{e^{\gamma_E}}{2} \right) \right] \left(\frac{\alpha_s}{\pi} \right)^2 , \\ D &= \frac{2}{3} \frac{\alpha_s}{\pi} \ln \left(\frac{e^{2\gamma_E-1}}{2} \right) , \end{aligned} \quad (4)$$

with $C_F = 4/3$ being a color factor, $f = 4$ the active flavor number, and γ_E the Euler constant. For the running coupling constant, we use

$$\alpha_s(\mu) = \frac{4\pi}{\beta_0 \ln(\mu^2/\Lambda_{\text{QCD}}^2)} \quad (5)$$

with $\beta_0 = (33 - 2f)/3$.

To get the transition elements of $B \rightarrow H$ ($H = K, K^*$) with various types of vertices, we parametrize them in terms of the relevant form factors as follows:

$$\langle K(P_2) | V_\mu | B(P_1) \rangle = F_1(q^2) P_\mu + F_2(q^2) q_\mu,$$

$$\begin{aligned}
\langle K(P_2) | T_{\mu\nu} q^\nu | B(P_1) \rangle &= F_T(q^2) (q^2 P_\mu - q \cdot P q_\mu), \\
\langle K^*(P_2, \varepsilon) | V_\mu | B(P_1) \rangle &= iV(q^2) \epsilon_{\mu\nu\alpha\beta} \varepsilon^{*\nu} P^\alpha q^\beta, \\
\langle K^*(P_2, \varepsilon) | A_\mu | B(P_1) \rangle &= A_0(q^2) \varepsilon_\mu^* + \varepsilon^* \cdot q [A_1(q^2) P_\mu + A_2(q^2) q_\mu], \\
\langle K^*(P_2, \varepsilon) | T_{\mu\nu} q^\nu | B(P_1) \rangle &= iT(q^2) \epsilon_{\mu\nu\alpha\beta} \varepsilon^{*\nu} P^\alpha q^\beta, \\
\langle K^*(P_2, \varepsilon) | T_{\mu\nu}^5 q^\nu | B(P_1) \rangle &= -T_0(q^2) \varepsilon_\mu^* - \varepsilon^* \cdot q [T_1(q^2) P_\mu + T_2(q^2) q_\mu], \quad (6)
\end{aligned}$$

with

$$T_0(q^2) + [T_1(q^2) P \cdot q + T_2(q^2) q^2] = 0 \quad (7)$$

where $V_\mu = \bar{s} \gamma_\mu b$, $A_\mu = \bar{s} \gamma_\mu \gamma_5 b$, $T_{\mu\nu} = \bar{s} i \sigma_{\mu\nu} b$, and $T_{\mu\nu}^5 = \bar{s} i \sigma_{\mu\nu} \gamma_5 b$. The correspondences of our notation to that usually used in the literature are shown in the Appendix. Using the PQCD factorization formula, the components of form factors defined in Eq. (6) are found to be

$$\begin{aligned}
F_1(q^2) &= -8\pi C_F M_B^2 \int_0^1 [dx] \int_0^\infty b_1 db_1 b_2 db_2 \phi_B(x_1, b_1) \\
&\quad \{ [r'_K (2\alpha_{2K} + 2\beta_{2K} - 1) \phi'_K(x_2, b_2) \\
&\quad - (1 + \beta_{2K} + (1 + 2r_K - s) \alpha_{2K}) \phi_K(x_2, b_2)] E_K(t_e^{(1)}) h^K(x_1, x_2, b_1, b_2) \\
&\quad + [-2r'_K (1 - \alpha_{1K} - \beta_{1K}) \phi'_K(x_2, b_2) \\
&\quad + (r_K (1 - \alpha_{1K} + \beta_{1K}) - s \beta_{1K}) \phi_K(x_2, b_2)] E_K(t_e^{(2)}) h^K(x_2, x_1, b_2, b_1) \} \quad (8)
\end{aligned}$$

$$\begin{aligned}
F_2(q^2) &= -8\pi C_F M_B^2 \int_0^1 [dx] \int_0^\infty b_1 db_1 b_2 db_2 \phi_B(x_1, b_1) \\
&\quad \{ [-r'_K (1 + 2\alpha_{2K} - 2\beta_{2K}) \phi'_K(x_2, b_2) + (1 + \beta_{2K} \\
&\quad + (1 + 2r_K - s) \alpha_{2K}) \phi_K(x_2, b_2)] E_K(t_e^{(1)}) h^K(x_1, x_2, b_1, b_2) \\
&\quad + [2r'_K (1 - \alpha_{1K} + \beta_{1K}) \phi'_K(x_2, b_2) + (r_K (1 - \alpha_{1K} - \beta_{1K}) \\
&\quad - (2 - s) \beta_{1K}) \phi_K(x_2, b_2)] E_K(t_e^{(2)}) h^K(x_2, x_1, b_2, b_1) \} \quad (9)
\end{aligned}$$

$$\begin{aligned}
F_T(q^2) &= -8\pi C_F M_B \int_0^1 [dx] \int_0^\infty b_1 db_1 b_2 db_2 \phi_B(x_1, b_1) \\
&\quad \times \{ [-\alpha_{2K} r'_K \phi'_K(x_2, b_2) + (1 - 2\beta_{2K}) \phi_K(x_2, b_2)] E_K(t_e^{(1)}) h^K(x_1, x_2, b_1, b_2) \\
&\quad + [2r'_K (1 - \alpha_{1K}) \phi'_K(x_2, b_2) - \beta_{1K} \phi_K(x_2, b_2)] E_K(t_e^{(2)}) h^K(x_2, x_1, b_2, b_1) \} \quad (10)
\end{aligned}$$

$$\begin{aligned}
V(q^2) &= 8\pi C_F M_B \int_0^1 [dx] \int_0^\infty b_1 db_1 b_2 db_2 \phi_B(x_1, b_1) \phi_{K^*}(x_2, b_2) \\
&\quad \times \{ [1 - 2\beta_{2K^*} - \sqrt{r_{K^*}} \alpha_{2K^*}] E_{K^*}(t_e^{(1)}) h^{K^*}(x_1, x_2, b_1, b_2) \\
&\quad + [\sqrt{r_{K^*}} (1 - \alpha_{1K^*})] E_{K^*}(t_e^{(2)}) h^{K^*}(x_2, x_1, b_2, b_1) \}, \quad (11)
\end{aligned}$$

$$\begin{aligned}
A_0(q^2) &= 8\pi C_F M_B^3 \int_0^1 [dx] \int_0^\infty b_1 db_1 b_2 db_2 \phi_B(x_1, b_1) \phi_{K^*}(x_2, b_2) \\
&\quad \times \{ [(1 + r_{K^*} - s) (1 - 2\beta_{2K^*} + \sqrt{r_{K^*}} \alpha_{2K^*}) \\
&\quad - 4r_{K^*} \alpha_{2K^*} + 2\sqrt{r_{K^*}} (1 + \beta_{2K^*})] E_{K^*}(t_e^{(1)}) h^{K^*}(x_1, x_2, b_1, b_2) \\
&\quad + \sqrt{r_{K^*}} [(1 + r_{K^*} - s) (1 - \alpha_{1K^*}) - 2\beta_{1K^*}] E_{K^*}(t_e^{(2)}) h^{K^*}(x_2, x_1, b_2, b_1) \} \quad (12)
\end{aligned}$$

$$\begin{aligned}
A_1(q^2) &= 8\pi C_F M_B \int_0^1 [dx] \int_0^\infty b_1 db_1 b_2 db_2 \phi_B(x_1, b_1) \phi_{K^*}(x_2, b_2) \\
&\quad \times \left\{ [-1 + 2\beta_{2K^*} + \sqrt{r_{K^*}} \alpha_{2K^*}] E_{K^*}(t_e^{(1)}) h^{K^*}(x_1, x_2, b_2, b_1) \right. \\
&\quad \left. + [\sqrt{r_{K^*}} (-1 + \alpha_{1K^*} + 2\beta_{1K^*})] E_{K^*}(t_e^{(2)}) h^{K^*}(x_2, x_1, b_1, b_2) \right\}, \tag{13}
\end{aligned}$$

$$\begin{aligned}
A_2(q^2) &= 8\pi C_F M_B \int_0^1 [dx] \int_0^\infty b_1 db_1 b_2 db_2 \phi_B(x_1, b_1) \phi_{K^*}(x_2, b_2) \\
&\quad \times \left\{ [1 - 2\beta_{2K^*} - \sqrt{r_{K^*}} \alpha_{2K^*}] E_{K^*}(t_e^{(1)}) h^{K^*}(x_1, x_2, b_1, b_2) \right. \\
&\quad \left. + [\sqrt{r_{K^*}} (1 - \alpha_{1K^*} + 2\beta_{1K^*})] E_{K^*}(t_e^{(2)}) h^{K^*}(x_2, x_1, b_2, b_1) \right\}, \tag{14}
\end{aligned}$$

$$\begin{aligned}
T(q^2) &= 8\pi C_F M_B^2 \int_0^1 [dx] \int_0^\infty b_1 db_1 b_2 db_2 \phi_B(x_1, b_1) \phi_{K^*}(x_2, b_2) \\
&\quad \times \left\{ [-(1 + \sqrt{r_{K^*}}) + 2s\alpha_{2K^*} + (2\sqrt{r_{K^*}} - 1)(\alpha_{2K^*} + \beta_{2K^*})] \right. \\
&\quad \times E_{K^*}(t_e^{(1)}) h^{K^*}(x_1, x_2, b_1, b_2) \\
&\quad \left. + \sqrt{r_{K^*}} [\alpha_{1K^*} + \beta_{1K^*}(x_1) - 1] E_{K^*}(t_e^{(2)}) h^{K^*}(x_2, x_1, b_2, b_1) \right\}, \tag{15}
\end{aligned}$$

$$\begin{aligned}
T_0(q^2) &= -8\pi C_F M_B^4 \int_0^1 [dx] \int_0^\infty b_1 db_1 b_2 db_2 \phi_B(x_1, b_1) \phi_{K^*}(x_2, b_2) \\
&\quad \times \left\{ [(1 - r_{K^*} - s)(1 + \beta_{2K^*}) + \sqrt{r_{K^*}}(1 - r_{K^*} + s) \right. \\
&\quad - 2\sqrt{r_{K^*}}((1 - r_{K^*})(\alpha_{2K^*} + \beta_{2K^*}) + s(\beta_{2K^*} - \alpha_{2K^*})) \\
&\quad - 2r_{K^*}\alpha_{2K^*} + (1 + r_{K^*} - s)(1 - s)\alpha_{2K^*}] E_{K^*}(t_e^{(1)}) h^{K^*}(x_1, x_2, b_1, b_2) \\
&\quad + \sqrt{r_{K^*}} [(1 - \alpha_{1K^*} - \beta_{1K^*})(1 - r_{K^*}) \\
&\quad \left. - s(1 + \beta_{1K^*} - \alpha_{1K^*})] E_{K^*}(t_e^{(2)}) h^{K^*}(x_2, x_1, b_2, b_1) \right\}, \tag{16}
\end{aligned}$$

$$\begin{aligned}
T_1(q^2) &= -8\pi C_F M_B^2 \int_0^1 dx_1 dx_2 \int_0^\infty b_1 db_1 b_2 db_2 \phi_B(x_1, b_1) \phi_{K^*}(x_2, b_2) \\
&\quad \times \left\{ [s\alpha_{2K^*} - (1 + \sqrt{r_{K^*}}) - (1 - 2\sqrt{r_{K^*}})(\alpha_{2K^*} + \beta_{2K^*})] \right. \\
&\quad \times E_{K^*}(t_e^{(1)}) h^{K^*}(x_1, x_2, b_1, b_2) \\
&\quad \left. - \sqrt{r_{K^*}} [1 - \alpha_{1K^*} - \beta_{1K^*}] E_{K^*}(t_e^{(2)}) h^{K^*}(x_2, x_1, b_2, b_1) \right\}, \tag{17}
\end{aligned}$$

$$\begin{aligned}
T_2(q^2) &= -8\pi C_F M_B^2 \int_0^1 dx_1 dx_2 \int_0^\infty b_1 db_1 b_2 db_2 \phi_B(x_1, b_1) \phi_{K^*}(x_2, b_2) \\
&\quad \times \left\{ [(2r_{K^*} - s)\alpha_{2K^*} + (1 + \alpha_{2K^*} + \beta_{2K^*}) \right. \\
&\quad - \sqrt{r_{K^*}}(1 + 2\alpha_{2K^*} - 2\beta_{2K^*})] E_{K^*}(t_e^{(1)}) h^{K^*}(x_1, x_2, b_1, b_2) \\
&\quad \left. + \sqrt{r_{K^*}} [1 - \alpha_{1K^*} + \beta_{1K^*}] E_{K^*}(t_e^{(2)}) h^{K^*}(x_2, x_1, b_2, b_1) \right\}, \tag{18}
\end{aligned}$$

where ϕ_B , ϕ_K (ϕ'_K), and ϕ_{K^*} are the wave functions of B , pseudovector (pseudoscalar) of K , and K^* mesons, respectively, the evolution factor are given by

$$E_H(t) = \alpha_s(t) \exp(-S_B(t) - S_H(t)), \tag{19}$$

and the related kinematic variables are parametrized as

$$\begin{aligned}
\alpha_{1H} &= -\frac{1}{\sqrt{\varphi_H}} x_1, & \beta_{1H} &= \frac{1}{2} \left(1 + \frac{1 + r_H - s}{\sqrt{\varphi_H}} \right) x_1, \\
\beta_{2H} &= -\frac{r_H}{\sqrt{\varphi_H}} x_2, & \alpha_{2H} &= \frac{1}{2} \left(1 + \frac{1 + r_H - s}{\sqrt{\varphi_H}} \right) x_2,
\end{aligned}$$

$$r_H = \frac{M_H^2}{M_B^2}, \quad r'_H = \frac{m_{0K}}{M_B}, \quad s = \frac{q^2}{M_B^2}, \quad (20)$$

with

$$\begin{aligned} \varphi_H &= (1 - r_H)^2 - 2s(1 + r_H) + s^2, \\ m_{0K} &= \frac{M_K^2}{m_s + m_d}. \end{aligned} \quad (21)$$

The hard functions, h^H , are written as

$$\begin{aligned} h^H(x_1, x_2, b_1, b_2) &= K_0(D_H \sqrt{x_1 x_2} b_1) [\theta(b_1 - b_2) K_0(D_H \sqrt{x_2} b_1) I_0(D_H \sqrt{x_2} b_2) \\ &\quad + \theta(b_2 - b_1) K_0(D_H \sqrt{x_2} b_2) I_0(D_H \sqrt{x_2} b_1)], \end{aligned} \quad (22)$$

with

$$D_H^2 = \frac{M_B^2}{2} \left(1 + r_H - \frac{q^2}{M_B^2} + \sqrt{\varphi_H} \right).$$

The derivation of h , from the Fourier transformation of the lowest-order hard decay amplitude, is similar to that for $B \rightarrow KK$ decays [14]. The hard scales $t^{(1,2)}$ are chosen by

$$\begin{aligned} t^{(1)} &= \max(\sqrt{x_2} D_H, 1/b_1, 1/b_2), \\ t^{(2)} &= \max(\sqrt{x_1} D_H, 1/b_1, 1/b_2). \end{aligned} \quad (23)$$

The wave functions ϕ_H and ϕ'_K are defined by [14, 17]

$$\begin{aligned} \phi_H(x) &= \int \frac{dy^+}{2\pi} e^{-ixP_3^- y^+} \frac{1}{2} \langle 0 | \bar{u}(y^+) \gamma^- \gamma_5 s(0) | H \rangle, \\ \frac{m_{0K}}{P_3^-} \phi'_K(x) &= \int \frac{dy^+}{2\pi} e^{-ixP_3^- y^+} \frac{1}{2} \langle 0 | \bar{u}(y^+) \gamma_5 s(0) | K \rangle, \end{aligned} \quad (24)$$

with the normalization conditions of

$$\int_0^1 dx \phi_B(x) = \int_0^1 dx \phi_H(x) = \int_0^1 dx \phi'_K(x) = \frac{f_{B(H)}}{2\sqrt{2}N_c}.$$

We note that unlike the kaon case, we do not distinguish the pseudovector and pseudoscalar components of the B wave functions since the factor $M_B/(m_b + m_d)$ is close to one. We also note that from Eqs. (15) and (17) we obtain $T(0) = -T_1(0)$.

3 Differential decay rates and lepton asymmetries

The effective Hamiltonian of $b \rightarrow s l^+ l^-$ is given by [20]

$$\mathcal{H} = \frac{G_F \alpha \lambda_t}{\sqrt{2}\pi} \left[C_8(\mu) \bar{s}_L \gamma_\mu b_L \bar{l} \gamma^\mu l + C_9 \bar{s}_L \gamma_\mu b_L \bar{l} \gamma^\mu \gamma_5 l - \frac{2m_b C_7(\mu)}{q^2} \bar{s}_L i \sigma_{\mu\nu} q^\nu b_R \bar{l} \gamma^\mu l \right] \quad (25)$$

where $C_8(\mu)$, C_9 and $C_7(\mu)$ are the WCs and their expressions can be found in Ref. [20] for the SM. Since the operator associated with C_9 is not renormalized under the QCD, it is the only one with the μ scale free. Besides the short-distance (SD) contributions, the main

effect on the branching ratio comes from $c\bar{c}$ resonant states such as $\Psi, \Psi' \dots etc.$, *i.e.*, the long-distance (LD) contributions. In the literature [21, 22, 23, 24, 25], it has been suggested by combining FA and vector meson dominance (VMD) approximation to estimate LD effects for the B decays. Hence, including the resonant effect (RE) and absorbing it to the related WC, we obtain the effective WC of C_8 as

$$C_8^{eff} = C_8(\mu) + (3C_1(\mu) + C_2(\mu)) \left(h(x, s) + \frac{3}{\alpha} \sum_{j=\Psi, \Psi'} k_j \frac{\pi \Gamma(j \rightarrow l^+ l^-) M_j}{q^2 - M_j^2 + i M_j \Gamma_j} \right), \quad (26)$$

where we have neglected the small Wilson coefficients, $h(x, s)$ describes the one-loop matrix elements of operators $O_1 = \bar{s}_\alpha \gamma^\mu P_L b_\beta \bar{c}_\beta \gamma_\mu P_L c_\alpha$ and $O_2 = \bar{s} \gamma^\mu P_L b \bar{c} \gamma_\mu P_L c$ [20], M_j (Γ_j) are the masses (widths) of intermediate states, and the factors k_j are phenomenological parameters for compensating the approximations of FA and VMD and reproducing the correct branching ratios $Br(B \rightarrow J/\Psi X \rightarrow l^+ l^- X) = Br(B \rightarrow J/\Psi X) \times Br(J/\Psi \rightarrow l^+ l^-)$. In this paper, for simplicity, we take $k_j = -1/(3C_1(\mu) + C_2(\mu))$.

Using Eqs. (6) and (25), the transition amplitudes of $B \rightarrow (K, K^*) l^+ l^-$ are as follows

$$\mathcal{M}_K = \frac{G_F \alpha \lambda_t}{2\sqrt{2}\pi} \left\{ \left[(F_1^8(q^2) - 2m_b F_T^7(q^2)) P_\mu \right] \bar{l} \gamma^\mu l + \left[F_1^9(q^2) P_\mu + F_2^9(q^2) q_\mu \right] \bar{l} \gamma^\mu \gamma_5 l \right\} \quad (27)$$

and

$$\begin{aligned} \mathcal{M}_{K^*} = & \frac{G_F \alpha \lambda_t}{2\sqrt{2}\pi} \left\{ i \left(V^8(q^2) - \frac{2m_b}{q^2} T^{7*}(q^2) \right) \epsilon_{\mu\nu\alpha\beta} \varepsilon^{*\nu} P^\alpha q^\beta \right. \\ & - \left(A_0^8(q^2) - \frac{2m_b}{q^2} T_0^7(q^2) \right) \varepsilon_\mu^* - \varepsilon^* \cdot q \left(A_1^8(q^2) - \frac{2m_b}{q^2} T_1^7(q^2) \right) P_\mu \left. \right] \bar{l} \gamma^\mu l \\ & + \left[i V^9(q^2) \epsilon_{\mu\nu\alpha\beta} \varepsilon^{*\nu} P^\alpha q^\beta - A_0^9(q^2) \varepsilon_\mu^* - \varepsilon^* \cdot q A_1^9(q^2) P_\mu \right] \bar{l} \gamma^\mu \gamma_5 l \left. \right\}. \quad (28) \end{aligned}$$

In Eqs. (27) and (28), we have included the WCs by inserting them into Eq. (19) as

$$E_H^j(t) = C_j(\mu) \alpha_s(t) \exp(-S_B(t) - S_H(t)) \quad (29)$$

and the superscripts of form factors denote the associated WCs of C_8^{eff} , C_9 , and C_7 , with the new definition of E_H^j in Eqs. (8)-(18), respectively.

As usual, after integrating the angle dependent phase space, the differential decay rates for $B \rightarrow H l^+ l^-$ ($H = K, K^*$) are found to be

$$\frac{d\Gamma_H(q^2)}{ds} = \frac{G_F^2 \alpha^2 |\lambda_t|^2 M_B^5}{3 \times 2^9 \pi^5} \sqrt{\varphi_H} \sqrt{1 - \frac{4m_l^2}{q^2}} \left[\left(1 + \frac{2m_l^2}{q^2} \right) \beta_H + 12 \frac{m_l^2}{M_B^2} \delta_H \right] \quad (30)$$

where

$$\beta_K = \varphi_K \left| F_1^8(q^2) - 2m_b F_T^7(q^2) \right|^2 + \varphi_K \left| F_1^9(q^2) \right|^2, \quad (31)$$

$$\delta_K = \left(1 + r_K - \frac{s}{2} \right) \left| F_1^9(q^2) \right|^2 + (1 - r_K) \text{Re} F_1^9(q^2) F_2^{9*}(q^2) + \frac{s}{2} \left| F_2^9(q^2) \right|^2, \quad (32)$$

$$\begin{aligned} \beta_{K^*} = & \left[s \left(2\varphi_{K^*} \tilde{V}(q^2) + 3\tilde{F}_0(q^2) \right) + \frac{\varphi_{K^*}}{4r_{K^*}} \left(\tilde{F}_0(q^2) + \varphi_{K^*} \tilde{F}_1(q^2) \right) \right. \\ & \left. + 2(1 - r_{K^*} - s) \tilde{F}_{01}(q^2) \right], \quad (33) \end{aligned}$$

$$\begin{aligned}
\delta_{K^*} = & \frac{\varphi_{K^*}}{2} \left[-2 |V^9(q^2) M_B|^2 - \frac{3}{\varphi_{K^*}} \left| \frac{A_0^9(q^2)}{M_B} \right|^2 + \frac{s}{4r_{K^*}} |A_2^9(q^2) M_B|^2 \right. \\
& + \frac{2(1+r_{K^*})-s}{4r_{K^*}} |A_1^9(q^2) M_B|^2 + \frac{1}{2r_{K^*}} \text{Re} \left(A_0^9(q^2) A_1^{9*}(q^2) + A_0^9(q^2) A_2^{9*}(q^2) \right) \\
& \left. + \frac{1-r_{K^*}}{2r_{K^*}} \text{Re} A_1^9(q^2) M_B A_2^{9*}(q^2) M_B \right], \tag{34}
\end{aligned}$$

with

$$\begin{aligned}
\tilde{V}(q^2) &= \left| V^8(q^2) M_B - \frac{2m_b M_B}{q^2} T^7(q^2) \right|^2 + |V^9(q^2) M_B|^2, \\
\tilde{F}_0(q^2) &= \left| \frac{A_0^8(q^2)}{M_B} - \frac{2m_b T_0^7(q^2)}{q^2 M_B} \right|^2 + \left| \frac{A_0^9(q^2)}{M_B} \right|^2, \\
\tilde{F}_1(q^2) &= \left| A_1^8(q^2) M_B - \frac{2m_b M_B}{q^2} T_1^7(q^2) \right|^2 + |A_1^9(q^2) M_B|^2, \\
\tilde{F}_{01}(q^2) &= \text{Re} \left[\left(\frac{A_0^8(q^2)}{M_B} - \frac{2m_b T_0^7(q^2)}{q^2 M_B} \right) \left(A_1^{8*}(q^2) M_B - \frac{2m_b M_B}{q^2} T_1^{7*}(q^2) \right) \right] \\
&+ \text{Re} \left(\frac{A_0^9(q^2)}{M_B} A_1^{9*}(q^2) M_B \right). \tag{35}
\end{aligned}$$

The forward-backward asymmetry (FBA) can be defined by

$$\mathcal{A}_{FB} = \frac{1}{d\Gamma(s)/ds} \left[\int_0^1 d\cos\theta \frac{d^2\Gamma(s)}{dsd\cos\theta} - \int_{-1}^0 d\cos\theta \frac{d^2\Gamma(s)}{dsd\cos\theta} \right], \tag{36}$$

where θ is the angle of charged l^+ with respect to the B meson in the rest frame of the lepton pair. For $B \rightarrow K^* l^+ l^-$ decay, the FBA is found to be

$$\mathcal{A}_{FB}^{K^*} = - \frac{3s\sqrt{\varphi_{K^*}}\sqrt{1-\frac{4m_l^2}{q^2}} R_{VA}(q^2)}{\left(1+\frac{2m_l^2}{q^2}\right)\beta_{K^*}+12\frac{m_l^2}{M_B^2}\delta_{K^*}} \tag{37}$$

with

$$\begin{aligned}
R_{VA}(q^2) &= \text{Re} \left[\left(V^8(q^2) M_B - \frac{2m_b M_B}{q^2} T^7(q^2) \right) \frac{A_0^{9*}(q^2)}{M_B} \right] \\
&+ \text{Re} \left[\left(\frac{A_0^8(q^2)}{M_B} - \frac{2m_b T_0^7(q^2)}{q^2 M_B} \right) V^{9*}(q^2) M_B \right]. \tag{38}
\end{aligned}$$

As expected, the FBA in Eq. (37) is sensitive to the chiral structure of interactions since it is related to the product of V and A currents. It is clear that the FBA for $B \rightarrow Kl^{+l^-}$ vanishes since there is no form factor from the axial current.

Another interesting lepton asymmetry is the longitudinal polarization of the lepton, defined by

$$P_L(q^2) = \frac{\frac{d\Gamma(n=-1)}{ds} - \frac{d\Gamma(n=1)}{ds}}{\frac{d\Gamma(n=-1)}{ds} + \frac{d\Gamma(n=1)}{ds}}$$

where n is the projection of the lepton l^- momentum to the spin direction in its rest frame. For $B \rightarrow (K, K^*) l^+ l^-$, the polarization asymmetries can be expressed as

$$P_L^K(q^2) = \frac{2\sqrt{1 - \frac{4m_l^2}{q^2}}\varphi_K}{\left(1 + \frac{2m_l^2}{q^2}\right)\beta_K + 12\frac{m_l^2}{M_B^2}\delta_K} \text{Re} \left[\left(F_1^8(q^2) - 2m_b F_T^7(q^2) \right) F_1^{9*}(q^2) \right] \quad (39)$$

and

$$P_L^{K^*}(q^2) = \frac{2\sqrt{1 - \frac{4m_l^2}{q^2}}}{\left(1 + \frac{2m_l^2}{q^2}\right)\beta_{K^*} + 12\frac{m_l^2}{M_B^2}\delta_{K^*}} \left\{ s \left[2\varphi_{K^*} R_V(q^2) + 3R_{A_0}(q^2) \right] + \frac{\varphi_{K^*}}{4r} \left[R_{A_0}(q^2) + \varphi_{K^*} R_{A_1}(q^2) + (1 - r_{K^*} - s) R_{A_{01}}(q^2) \right] \right\} \quad (40)$$

with

$$\begin{aligned} R_V(q^2) &= \text{Re} \left[\left(V^8(q^2) M_B - \frac{2m_b M_B}{q^2} T^7(q^2) \right) V^{9*}(q^2) M_B \right], \\ R_{A_0}(q^2) &= \text{Re} \left[\left(\frac{A_0^8(q^2)}{M_B} - \frac{2m_b T_0^7(q^2)}{q^2 M_B} \right) \frac{A_0^{9*}(q^2)}{M_B} \right], \\ R_{A_1}(q^2) &= \text{Re} \left[\left(A_1^8(q^2) M_B - \frac{2m_b M_B}{q^2} T_1^7(q^2) \right) A_1^{9*}(q^2) M_B \right], \\ R_{A_{01}}(q^2) &= \text{Re} \left[\left(\frac{A_0^8(q^2)}{M_B} - \frac{2m_b T_0^7(q^2)}{q^2 M_B} \right) A_1^{9*}(q^2) M_B \right. \\ &\quad \left. + \left(A_1^8(q^2) M_B - \frac{2m_b M_B}{q^2} T_1^7(q^2) \right) \frac{A_0^{9*}(q^2)}{M_B} \right], \end{aligned} \quad (41)$$

respectively.

4 Numerical Analysis

4.1 Form factors

In Eq. (1), $\phi(x, b)$ is the universal wave function and cannot be calculated perturbatively. However, due to the universality, we can determine it by matching with the B decay experimental data. With the ratio of

$$R = \frac{B(B_d^0 \rightarrow K^\pm \pi^\mp)}{B(B^\pm \rightarrow K^0 \pi^\pm)} = 0.95 \pm 0.3, \quad (42)$$

given by the CLEO measurement [26], where $B(B_d^0 \rightarrow K^\pm \pi^\mp)$ represents the CP average of the branching ratios $B(B_d^0 \rightarrow K^+ \pi^-)$ and $B(\bar{B}_d^0 \rightarrow K^- \pi^+)$, one can get the proper wave functions ϕ_B , ϕ_K , and ϕ'_K [17] while ϕ_{K^*} can be done by the branching ratio of $B \rightarrow K^* \gamma$ [13]. For the B meson wave function, we take

$$\phi_B(x, b) = N_B x^2 (1-x)^2 \exp \left[-\frac{1}{2} \left(\frac{x M_B}{\omega_B} \right)^2 - \frac{\omega_B^2 b^2}{2} \right], \quad (43)$$

with the shape parameter $\omega_B = 0.4$ GeV [27]. The normalization constant $N_B = 91.7835$ GeV is related to the decay constant $f_B = 190$ MeV. The kaon wave functions are chosen as

$$\begin{aligned}\phi_K(x) &= \frac{3}{\sqrt{2N_c}} f_K x(1-x)[1 + 0.51(1-2x) + 0.3(5(1-2x)^2 - 1)], \\ \phi'_K(x) &= \frac{3}{\sqrt{2N_c}} f_K x(1-x), \\ \phi_{K^*}(x) &= \frac{3}{\sqrt{2N_c}} f_{K^*} x(1-x)[1 + 0.51(1-2x) + (5(1-2x)^2 - 1)],\end{aligned}\quad (44)$$

where ϕ_K is derived from QCD sum rules [28], and the second term in the expression of ϕ_K corresponds to $SU(3)$ symmetry breaking effect. The decay constants f_K and f_{K^*} are set to be 160 and 190 MeV (in the convention of $f_\pi = 130$ MeV), respectively. Note that the intrinsic b dependences of wave functions in Eq. (44) are neglected. However, this is a good approximation only for the fast recoiling meson, that is, the transverse extent of the wave function is less important in the energetic outgoing situation. With above wave functions and taking $M_B = 5.28$ GeV, $M_K = 0.49$ GeV, $m_s = 100$ MeV and $M_{K^*} = 0.89$ GeV, the form factors of $B \rightarrow K$ defined in Eqs. (6) as a function of q^2 are shown in Figure 1. The values of the form factors at $q^2 = 0$ are given in Table 1. We now compare our results with that in the light cone-QCD sum rule (LCSR) [2]. Using the identities in the Appendix, we find that except $V(0)$ is slightly smaller than that of the minimal value, while the remaining form factors are within the allowed values, in the LCSR. Recently, it has been

Table 1: Form factors at $q^2 = 0$ in the PQCD.

$F_1(0)$	$F_2(0)$	$F_T(0)$	$V(0)$	$A_0(0)$	$A_1(0)$	$A_2(0)$	$T(0)$	$T_1(0)$	$T_2(0)$
0.33	-0.267	-0.054	0.063	2.02	-0.05	0.059	-0.350	0.350	-0.281

mentioned that by combining large energy effective theory (LEET) [19], originally proposed by [18], with the measurement of $B \rightarrow K^* \gamma$, the form factors $V(0)$ and $A_0(0)$ could be fitted model-independently to be [32]

$$\begin{aligned}V(0) &\simeq 0.069 \pm 0.011, \\ A_0(0) &\simeq 1.650 \pm 0.114.\end{aligned}\quad (45)$$

Hence, from Table 1, we clearly see that the values of $V(0)$ and $A_0(0)$ are within 1σ and 3.2σ of values in Eq. (45), respectively. It is worth to mention that the LEET predicts $T_2(0)/A_1(0) \sim 4.89$ [32], while that in our approach is 5.62. For the comparison of the form factors between different models at $q^2 = 0$, one can refer to Ref. [32] for a more detail analysis.

For the exclusive $B \rightarrow K^{(*)} l^+ l^-$ decays, if we use b independent wave functions, as the mesons reach the slow recoil, the suppression in the large b region is weaker such that form factors will blow up at points away from $q^2 = 0$ as seen from Figure 1. It is inevitable to include the intrinsic b dependence to the outgoing meson wave functions. However, the effect of such dependence is less significant for the small q^2 values than that of large ones. Instead of using an exponential b dependent form as the one for the B meson wave function in Eq. (43), for simplicity, we use the trial wave functions as

$$\phi_H^{(l)}(x, q^2) = \left(1 - \frac{q^2}{M_B^2}\right) \sqrt{1 + \frac{q^2}{M_B^2}} \phi_H^{(l)}(x). \quad (46)$$

On the other hand, since the available region of the PQCD essentially cannot include all allowed values of q^2 , to have the form factors in the whole accessible values of q^2 , we would adopt the parametrization of effective form factors as follows:

$$F(s) = F(0) \exp\left(\sigma_1 s + \sigma_2 s^2 + \sigma_3 s^3\right) \quad (47)$$

with $s = q^2/M_B^2$ to fit the values up to $q^2 \approx 15 \text{ GeV}^2$ calculated by the PQCD. By extrapolating to near the endpoint of q^2 , we found that the values of form factors are consistent with lattice results [29, 30]. To illustrate how good the trial functions in Eq. (46) are, we show the form factors for $B \rightarrow K$ in Figure 2. From the figure, we find that our results are basically the same as that from the QM [31] and LCSR [2].

4.2 Decay rates

With the confidence of calculating the form factors by using Eqs. (46) and (47), we now study the decay rates of $B \rightarrow K^{(*)}l^+l^-$. Unlike the conventional FA, the WCs in Eqs. (27) and (28) are the members of integrations in the PQCD. Thus, adopting the approach similar to form factors, we calculate the transition amplitudes with the wave functions in Eq. (46) and the exponential forms in Eq. (47) to fit the values calculated by the PQCD for the whole range of q^2 . After integrating q^2 dependence in Eq. (30), the decay branching ratios without including LD contributions for $B \rightarrow (K, K^*)l^+l^-$ are listed in Table 2 and their distributions for the differential decay rates are shown in Figure 3. Comparing with the curves in the QM and LCSR, we find that the differential rates of $B \rightarrow Kl^+l^-$ are consistent with each other. However, there exists a slight difference in $B \rightarrow K^*l^+l^-$. There are two main reasons for the difference: (a) μ scale dependence for the WC and (b) the effects from $A_1(q^2)$ and $A_2(q^2)$ in the PQCD. For the results in QM and LCSR, we have used the WC at $\mu \sim m_b$ as done in the literature, whereas that in the PQCD, μ scale is the typical scale t determined by Eq. (23). As seen from Eq. (35) the effect of $A_1(q^2)$ is large since there is a factor of M_B associated with it, while that of $A_2(q^2)$ only affects in the mode of $B \rightarrow K^*\tau^+\tau^-$ due to the lepton mass dependence. Thus, measuring the exclusive modes of $B \rightarrow K^*l^+l^-$ would distinguish various QCD models due to the difference shown in Figure 3. From Table 2, we see that our PQCD results of the decay branching ratios for $B \rightarrow K^*\mu^+\mu^-$ and $B \rightarrow K^*e^+e^-$ are quite different. This can be understood by noting that in Eq. (33) there is pole of q^2 associated with the photon penguin induced couplings. These pole terms make the rates sensitive to the kinematical region of $q^2 \geq 4m_l^2$.

4.3 Forward-backward asymmetry

From Eq. (37), we present the forward-backward dilepton asymmetries of $B \rightarrow K^*l^+l^-$ ($l = \mu, \tau$) in Figure 4. We note that the FBA of $B \rightarrow K^*e^+e^-$ is similar to that of the muon mode in Figure 4. For the light lepton pair decays such as $B \rightarrow K^*\mu^+\mu^-$, we see that the FBA is positive at low q^2 , gets zero at $q^2/M_B^2 \sim 0.16$, and then becomes negative. Due to the large terms related to $A_1(q^2)$, the rate at lower q^2 in the PQCD has a larger value than that in the QM and LCSR. As mentioned in Ref. [2] with the FA, the location of zero point

Table 2: Decay branching ratios in the various QCD models without including LD effects.

Mode	PQCD	QM	LCSR
$10^7 \text{B}(B \rightarrow Kl^+l^-)$	5.33	5.56	5.20
$10^7 \text{B}(B \rightarrow K\tau^+\tau^-)$	1.29	1.28	1.25
$10^6 \text{B}(B \rightarrow K^*e^+e^-)$	2.26	1.88	2.23
$10^6 \text{B}(B \rightarrow K^*\mu^+\mu^-)$	1.27	1.49	1.78
$10^7 \text{B}(B \rightarrow K^*\tau^+\tau^-)$	1.24	1.43	1.77

is only sensitive to the WC and insensitive to the form factors. However, since with the three-scale factorization formula the WC cannot be factored out of the transition amplitude and it is uncertain to choose the universal wave function of K^* , the determination of zero point is harder as the test of the SM in the approach of the PQCD, unless we can fix K^* wave function more precisely. On the other hand, it is worth to mention that when the $\text{sign}(C_8C_7) = +$, opposite to the SM, the zero point disappears. Thus the FBA is quite sensitive to the sign of the WC and can be used as a good candidate to test the SM.

4.4 Polarization asymmetry

The lepton polarization asymmetries of $B \rightarrow (K, K^*)l^+l^-$ are displayed in Figure 5. For $B \rightarrow Kl^+l^-$, P_L is equal zero at $q^2 = 0$ and $q^2|_{\text{max}} = (M_B - M_K)^2$ because it is related to $\sqrt{1 - 4m_l^2/q^2}\varphi_K$. Without LD effects for the light leptons ($l = e, \mu$), from Eqs. (31) and (39), we easily realize that P_L is near -1 in the most region of q^2 . However, for $B \rightarrow K^*l^+l^-$, since φ_{K^*} cannot be factored out in the numerator, there is no vanishing point at $q^2|_{\text{max}}$; and the transition matrix elements of the set $\{T^7\}$ are always associated with a pole of q^2 . Hence, at the low momentum transfer region, penguin induced electromagnetic effects are dominant. Also comparing Eq. (40) with Eq. (33), the related terms of $\{T^7\}$ are two powers for the differential decay rate but only one power for the numerator of P_L so that the magnitude of the distribution at low q^2 has a smaller value. From Figures 5c and 5d, the polarization asymmetry of $B \rightarrow K^*\mu^+\mu^-$ in the PQCD has slightly different distribution to other models at low q^2 , especially that the deviation for $B \rightarrow K^*\tau^+\tau^-$ is large. However, according to Figure 6, we find that our results are comparable with that given by the light-front formalism (LF) [33, 34]. As mentioned before, the influence of both larger values from the $A_1(q^2)$ and $A_2(q^2)$ terms in our approach is visible for the τ mode. Therefore, by measuring the longitudinal τ polarization in $B \rightarrow K^*\tau^+\tau^-$, we can either determine a more proper K^* wave function or test the feasibility of our PQCD approach for semileptonic decays.

5 Conclusions

By the three-scale factorization theorem, we have gotten the form factors in $q^2 \leq 15 \text{ GeV}^2$; and with the parametrization in terms of the exponential forms to extrapolate the q^2 dependent form factors to q_{max}^2 , we have obtained the consistent results with that from the lattice [29, 30]. With the PQCD, we have pointed out that the largest uncertainty in our results

is from the non-perturbative wave functions. Though the universal wave function could be determined by some non-leptonic decays, the intrinsic b dependence which suppresses the soft dynamics contribution is still unknown.

With the kaon wave functions fixed by the decays of $B \rightarrow \pi K$ and assumed q^2 dependences, we have shown that the distributions of the decay rates and leptonic asymmetries for $B \rightarrow Kl^+l^-$ in the PQCD agree well with that in the other QCD models such as the QM and LCSR. However, there are some differences for that in $B \rightarrow K^*l^+l^-$ among the various QCD models. Finally, we remark that although $B \rightarrow K^*\gamma$ could also give us some information of the K^* wave function, one still cannot fix it satisfactorily due to various uncertainties in the decay. Moreover, the assumption of the same q^2 dependent factors in $B \rightarrow K$ is not necessary for $B \rightarrow K^*$ and thus, to have a reliable calculation, we need more precision measurements involving the vector kaon meson in order to settle down the K^* wave function.

Acknowledgments

We would like to thank Hsiang-nan Li for useful discussions. This work was supported in part by the National Science Council of the Republic of China under contract numbers NSC-89-2112-M-007-054 and NSC-89-2112-M-006-033.

Appendix

In order to connect our form factors in Eq. (6) to those usually used in the literature [2, 31, 32, 33], in this Appendix we show explicitly the relationships among the form factors. In terms of the notation in Refs. [2, 32], the form factors for $B \rightarrow (K, K^*)$ decays with respect to various weak currents are parametrized as

$$\begin{aligned} \langle K(P_2) | V_\mu | B(P_1) \rangle &= f_+(q^2) \left(P_\mu - \frac{P \cdot q}{q^2} q_\mu \right) \\ &\quad + \frac{P \cdot q}{q^2} f_0(q^2) q_\mu, \end{aligned} \quad (48)$$

$$\langle K(P_2) | T_{\mu\nu} q^\nu | B(P_1) \rangle = - (P_\mu q^2 - q_\mu P \cdot q) f_T(q^2), \quad (49)$$

$$\langle K^*(P_2, \varepsilon) | V_\mu | B(P_1) \rangle = - \frac{V'(q^2)}{M_B + M_{K^*}} \epsilon_{\mu\nu\alpha\beta} \varepsilon^{*\nu} P^\alpha q^\beta, \quad (50)$$

$$\begin{aligned} \langle K^*(P_2, \varepsilon) | A_\mu | B(P_1) \rangle &= i2M_{K^*} A'_0(q^2) \frac{\varepsilon^* \cdot q}{q^2} q_\mu \\ &\quad + i(M_B + M_{K^*}) A'_1(q^2) \left(\varepsilon^{*\mu} - \frac{\varepsilon^* \cdot q}{q^2} q_\mu \right) \\ &\quad - iA'_2(q^2) \frac{\varepsilon^* \cdot q}{M_B + M_{K^*}} \left(P_\mu - \frac{P \cdot q}{q^2} q_\mu \right), \end{aligned} \quad (51)$$

$$\langle K^*(P_2, \varepsilon) | T_{\mu\nu} q^\nu | B(P_1) \rangle = T'_1(q^2) \epsilon_{\mu\nu\alpha\beta} \varepsilon^{*\nu} P^\alpha q^\beta, \quad (52)$$

$$\begin{aligned} \langle K^*(P_2, \varepsilon) | T_{\mu\nu}^5 q^\nu | B(P_1) \rangle &= iT'_2(q^2) \left[\varepsilon_\mu^* P \cdot q + \varepsilon^* \cdot q P_\mu \right] \\ &\quad - iT'_3(q^2) \varepsilon^* \cdot q \left[q_\mu - \frac{q^2}{P \cdot q} P_\mu \right], \end{aligned} \quad (53)$$

where $V_\mu = \bar{s} \gamma_\mu b$, $A_\mu = \bar{s} \gamma_\mu \gamma_5 b$, $T_{\mu\nu} = \bar{s} i\sigma_{\mu\nu} b$, $T_{\mu\nu}^5 = \bar{s} i\sigma_{\mu\nu} \gamma_5 b$, $P = P_1 + P_2$, $q = P_1 - P_2$, and $P \cdot q = M_B^2 - M_{K^*}^2$. Redefining the wave functions and comparing to Eq. (6), we obtain

$$\begin{aligned} F_1 &= f_+ \\ F_2 &= \frac{M_B^2 - M_{K^*}^2}{q^2} (f_0 - f_+) \\ V &= \frac{V'}{M_B + M_{K^*}} \\ A_0 &= (M_B + M_{K^*}) A'_1 \\ A_1 &= - \frac{A'_2}{M_B + M_{K^*}} \\ A_2 &= \frac{1}{q^2} [2M_{K^*} A'_0 - (M_B + M_{K^*}) A'_1 + (M_B - M_{K^*}) A'_2] \\ T &= -T'_1 \\ T_0 &= - (M_B^2 - M_{K^*}^2) T'_2 \\ T_1 &= T'_2 + \frac{q^2}{M_B^2 - M_{K^*}^2} T'_3 \\ T_2 &= -T'_3. \end{aligned}$$

Here we have neglected to show the q^2 dependence for the form factors. From the above identities, we find some interesting relations at $q^2 = 0$ and they are given by

$$\begin{aligned} f_0(0) &= f_+(0), \\ T_1(0) &= T_2'(0). \end{aligned}$$

From Eqs. (15) and (17), we get $T(0) = -T_1(0)$. Hence, based on the modified PQCD factorization theorem, we obtain the relation $T_1'(0) = T_2'(0)$ that is the same as that in Eq. (3.6) of Ref. [2].

References

- [1] CLEO Collaboration, M. S. Alam et. al., Phys. Rev. Lett. **74**, 2885 (1995).
- [2] For a recent review, see A. Ali, P. Ball, L.T. Handoko, and G. Hiller, Phys. Rev. **D61**, 074024 (2000); and references therein.
- [3] N. Cabibbo, Phys. Rev. Lett. **10**, 531 (1963); M. Kobayashi and T. Maskawa, Prog. Theor. Phys. **49**, 652 (1973).
- [4] S. Brodsky and P. Lepage, Phys. Lett. **B87**, 959 (1979); Phys. Rev. **D22**, 2157 (1980).
- [5] A. Szczepaniak, E. M. Henley, and S. Brodsky, Phys. Lett. **B243**, 287 (1990).
- [6] G. Burdman and J.F. Donoghue, Phys. Lett. **B270**, 55 (1991).
- [7] N. Isgur and C.H. Llewellyn Smith, Phys. Rev. Lett. **52**, 1080 (1984); Phys. Lett. **B217**, 535 (1989); Nucl. Phys. **B317**, 526 (1989).
- [8] A.V. Radyushkin, Nucl. Phys. **A532**, 141 (1991).
- [9] H-n. Li and G. Sterman, Nucl. Phys. **B381**, 129 (1992).
- [10] T.W. Yeh and H-n. Li, Phys. Rev. **D56**, 1615 (1997).
- [11] H-n. Li and H.L. Yu, Phys. Rev. Lett. **74**, 4388 (1995); Phys. Lett. **B353**, 301 (1995); Phys. Rev. **D53**, 2480 (1996).
- [12] C.H. Chang and H-n. Li, Phys. Rev. **D55**, 5577 (1997) .
- [13] H-n. Li and G.L. Lin, Phys. Rev. **D60**, 054001 (1999).
- [14] C.H. Chen and H-n. Li, Phys. Rev. **D63**, 014003 (2000).
- [15] J.C. Collins and D.E. Soper, Nucl. Phys. **B193**, 381 (1981).
- [16] J. Botts and G. Sterman, Nucl. Phys. **B325**, 62 (1989).
- [17] Y.Y. Keum, H-n. Li and A.I. Sanda, hep-ph/0004004; hep-ph/0004173.
- [18] M. Dugan and B. Grinstein, Phys. Lett. **B255**, 583 (1991).
- [19] J. Charles, A.L. Yaouanc, L. Oliver, O. Pène, and J.C. Raynal, Phys. Rev. **D60**, 014001 (1999).
- [20] G. Buchalla, A. J. Buras and M. E. Lautenbacher, Rev. Mod. Phys. **68**, 1230 (1996).
- [21] N.G. Deshpande, J. Trampetic and K. Panose, Phys. Rev. **D39**, 1462 (1989).
- [22] C.S. Lim, T. Morozumi, and A.T. Sanda, Phys. Lett. **B218**, 343 (1989).
- [23] A. Ali, T. Mannel, and T. Morozumi, Phys. Lett. **B273**, 505 (1991).
- [24] P.J. O'Donnell and K.K.K. Tung, Phys. Rev. **D43**, R2067 (1991).

- [25] F. Krüger and L.M. Sehgal, Phys. Lett. **B380**, 199 (1996).
- [26] CLEO Coll., D. Cronin-Hennessy et al., hep-ex/0001010.
- [27] M. Bauer and M. Wirbel, Z. Phys. C **42**, 671 (1998).
- [28] P. Ball, JHEP 9809, 005 (1998).
- [29] APE Collaboration, A. Abada *et al.*, Phys. Lett. **B365**, 275 (1996).
- [30] UKQCD Collaboration, L. Del Debbio *et al.* Phys. Lett. **B416**, 392 (1998).
- [31] D. Melikhov, N. Nikitin, and S. Simula, Phys. Rev. D**57**, 6814 (1998).
- [32] G. Burdman and G. Hiller, hep-ph/0011266.
- [33] W. Jaus and D. Wyler, Phys. Rev. D**41**, 3405 (1990); C. Greub, A.Ioannissian and D. Wyler, Phys. Lett. **B346**, 149 (1995).
- [34] C.Q. Geng and C.P. Kao, Phys. Rev. D**54**, 5636 (1996).

Figure Captions

- Figure 1: Form factors of F_1 (solid curves), F_2 (dashed curves) and F_T (dotted curves) for the $B \rightarrow K$ transition as a function q^2 in the PQCD (bold lines) and QM (un-bold lines), respectively.
- Figure 2: Form factors of F_1 , F_2 and F_T for the $B \rightarrow K$ transition as a function q^2 with the q^2 dependent wave function in Eq. (46) in the PQCD (solid curves), QM (dot-dashed curves), and LCSR (dashed curves), respectively.
- Figure 3: The differential decay braching ratios as function of s for (a) $B \rightarrow K\mu^+\mu^-$ and (b) $B \rightarrow K\tau^+\tau^-$. The curves with and without resonant shapes represent including and no LD contributions, respectively. Legend is the same as Figure 2.
- Figure 4: The differential decay braching ratios as function of s for (a) $B \rightarrow K^*\mu^+\mu^-$ and (b) $B \rightarrow K^*\tau^+\tau^-$. Legend is the same as Figure 3.
- Figure 5: Forward-backward asymmetries for (a) $B \rightarrow K^*\mu^+\mu^-$ and (b) $B \rightarrow K^*\tau^+\tau^-$. Legend is the same as Figure 3.
- Figure 6: Longitudinal polarization asymmetries for (a) $B \rightarrow K\mu^+\mu^-$ and (b) $B \rightarrow K\tau^+\tau^-$. Legend is the same as Figure 3.
- Figure 7: Longitudinal polarization asymmetries (a) $B \rightarrow K^*\mu^+\mu^-$ and (b) $B \rightarrow K^*\tau^+\tau^-$. Legend is the same as Figure 3.
- Figure 8: The longitudinal polarization asymmetry for $B \rightarrow K^*\tau^+\tau^-$ in the PQCD (solid curves) and LF (dashed curves), respectively.

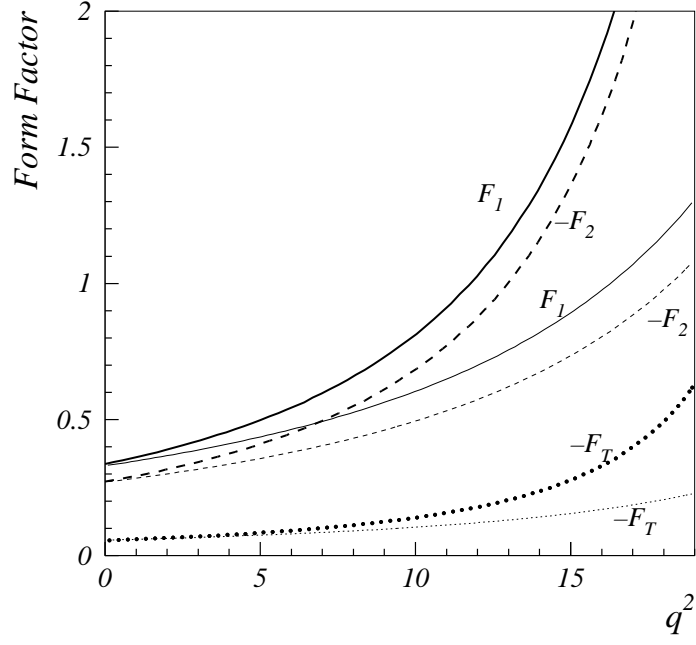


Figure 1: Form factors of F_1 (solid curves), F_2 (dashed curves) and F_T (dotted curves) for the $B \rightarrow K$ transition as a function q^2 in the PQCD (bold lines) and QM (un-bold lines), respectively.

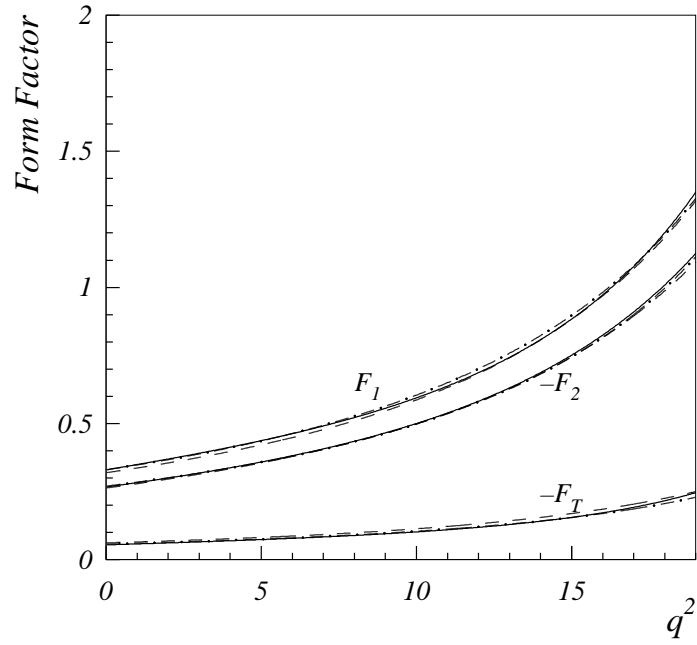


Figure 2: Form factors of F_1 , F_2 and F_T for the $B \rightarrow K$ transition as a function q^2 with the q^2 dependent wave function in Eq. (46) in the PQCD (solid curves), QM (dot-dashed curves), and LCSR (dashed curves), respectively.

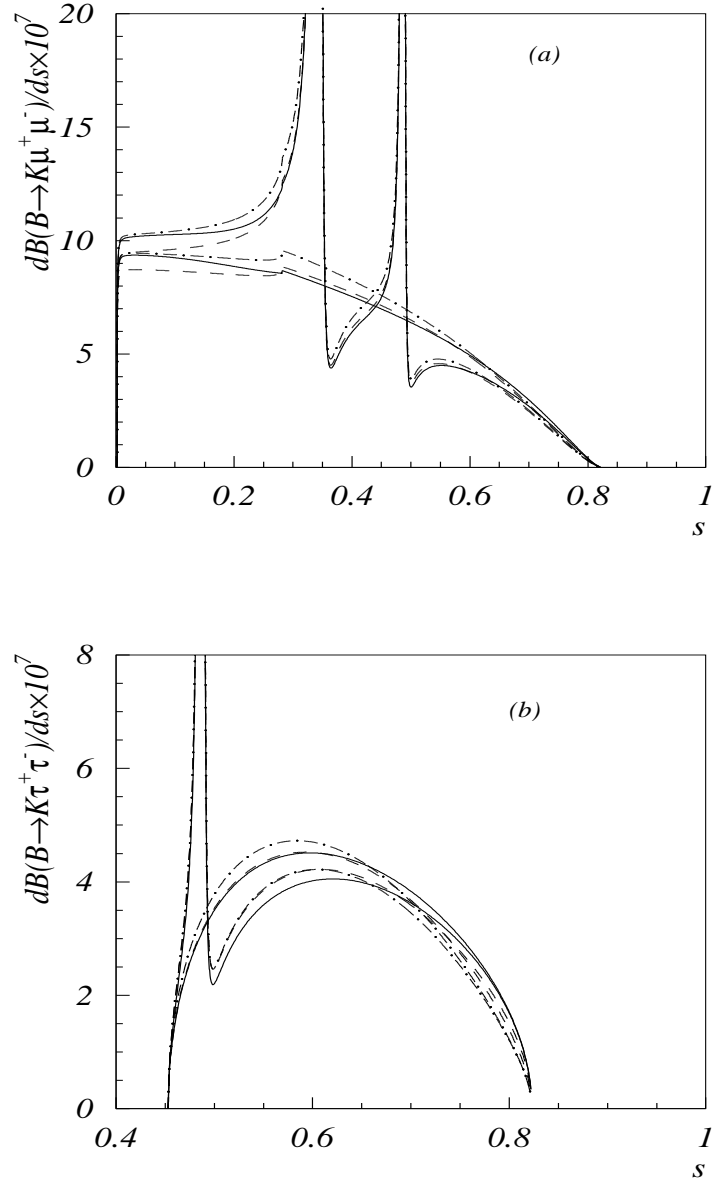


Figure 3: The differential decay branching ratios as function of s for (a) $B \rightarrow K\mu^+\mu^-$ and (b) $B \rightarrow K\tau^+\tau^-$. The curves with and without resonant shapes represent including and no LD contributions, respectively. Legend is the same as Figure 2.

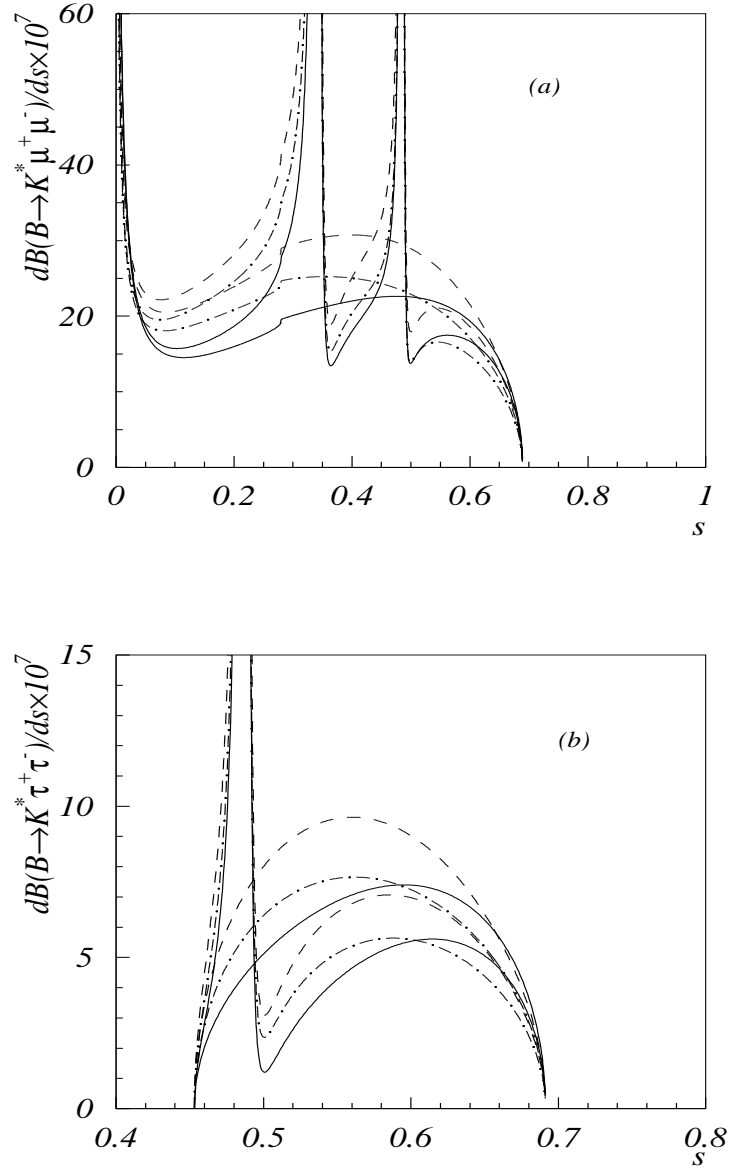


Figure 4: The differential decay branching ratios as function of s for (a) $B \rightarrow K^* \mu^+ \mu^-$ and (b) $B \rightarrow K^* \tau^+ \tau^-$. Legend is the same as Figure 3.

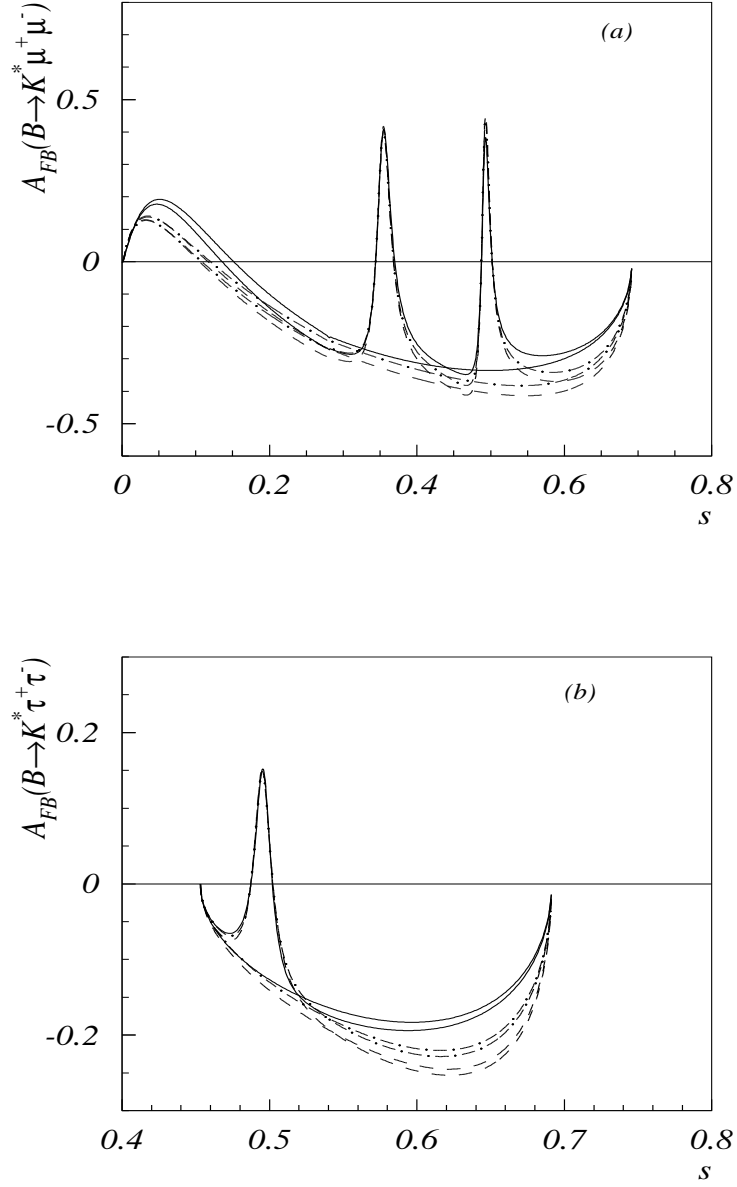


Figure 5: Forward-backward asymmetries for (a) $B \rightarrow K^* \mu^+ \mu^-$ and (b) $B \rightarrow K^* \tau^+ \tau^-$. Legend is the same as Figure 3.

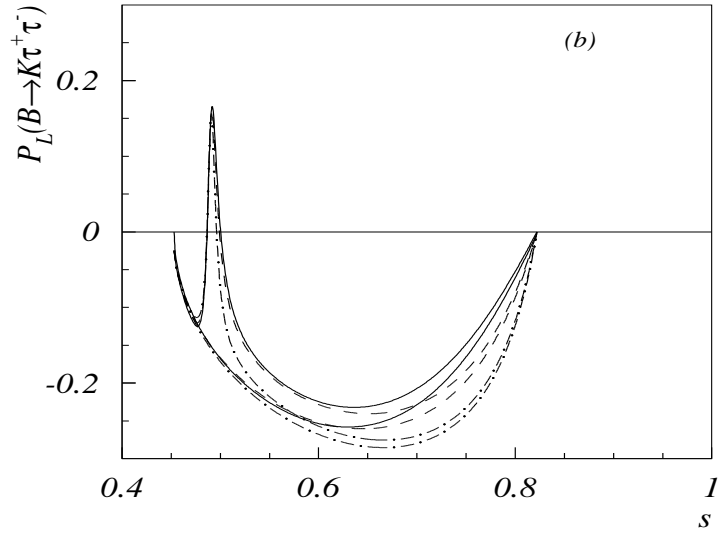
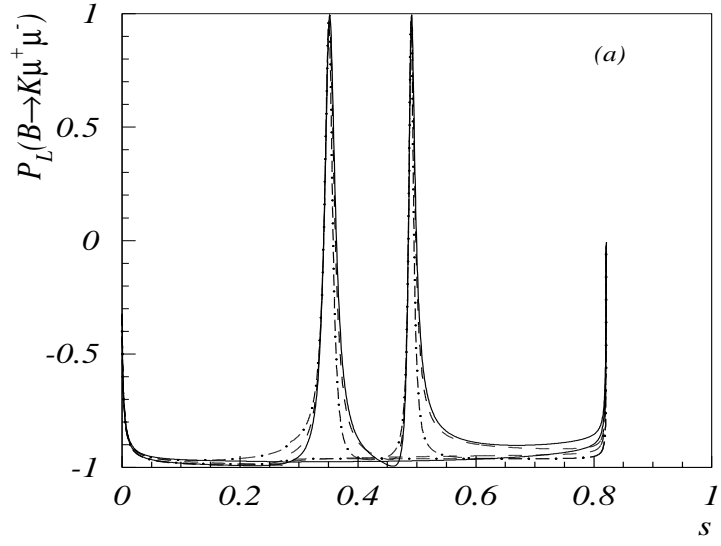


Figure 6: Longitudinal polarization asymmetries for (a) $B \rightarrow K\mu^+\mu^-$ and (b) $B \rightarrow K\tau^+\tau^-$. Legend is the same as Figure 3.

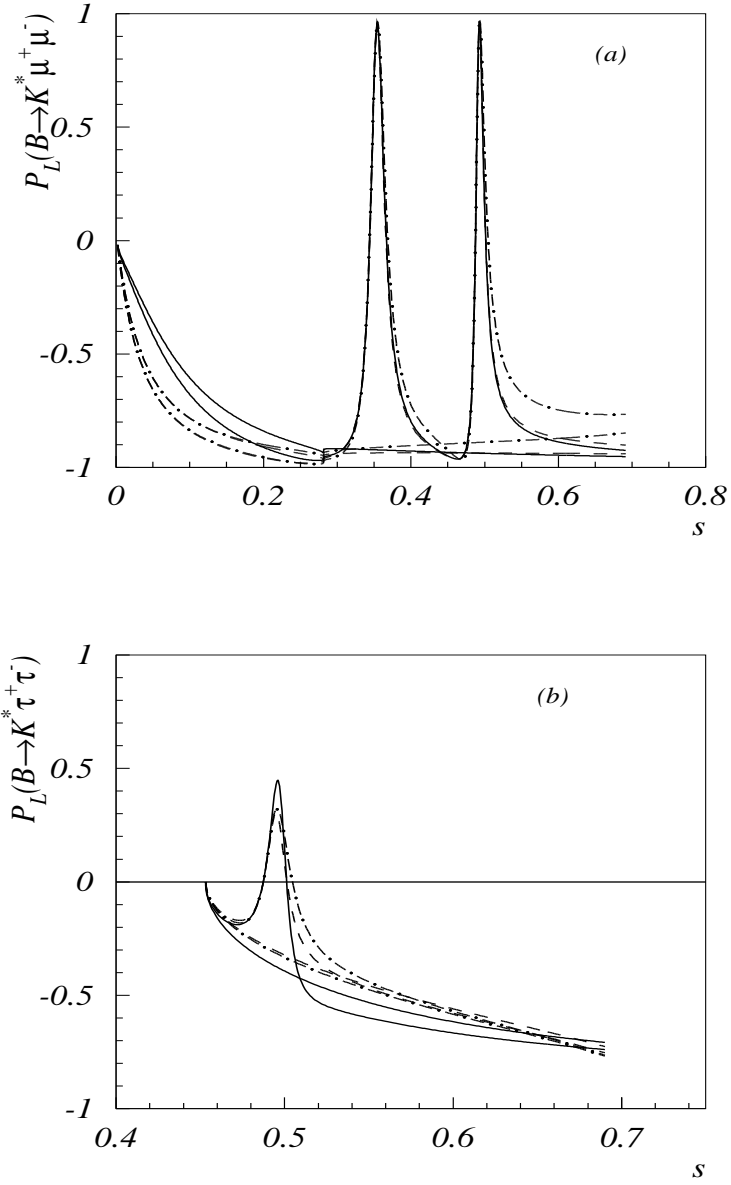


Figure 7: Longitudinal polarization asymmetries (a) $B \rightarrow K^* \mu^+ \mu^-$ and (b) $B \rightarrow K^* \tau^+ \tau^-$. Legend is the same as Figure 3.

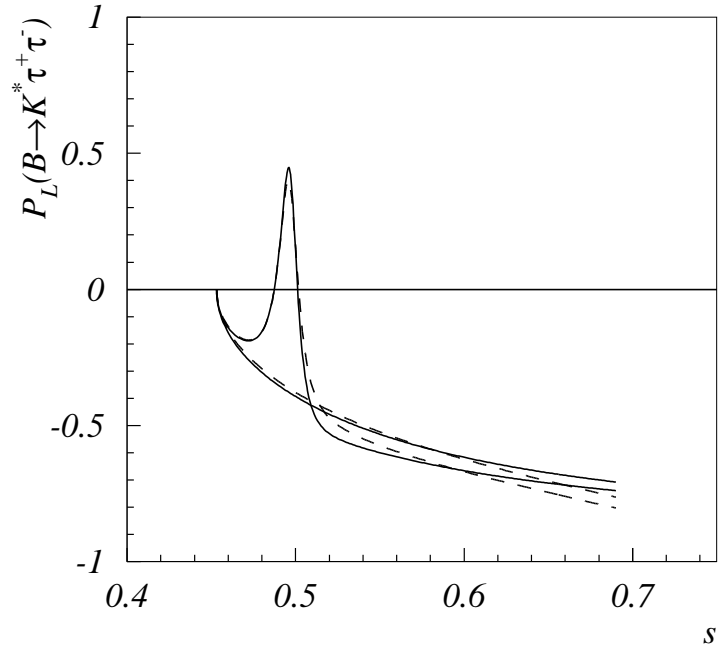


Figure 8: The longitudinal polarization asymmetry for $B \rightarrow K^* \tau^+ \tau^-$ in the PQCD (solid curves) and LF (dashed curves), respectively.